RoboBoat 2026: Technical Design Report

Team DoB JolJan

Dreams of Bangladesh

MD. Moin Uddin, MD Mubassirul Islam, Mahadir Islam, Mahadi Hassan, Tamim Hossain, Ahnaf Safwan Islam, Kamrul Islam, Al Amin Sani, Dewan MD Foyzullah Munim, Abrar Atif Rahman, MD Asadullah Sami, Anas Bin Azim, Samin Yaser, Mohammad Sifat, Mohammad Nowfil Aziz, Ayaan Islam Ariyan, Ishmam Tahsan Masafi

Abstract—Jolojan is debuting a new autonomous surface vehicle (ASV), *Jolorekha*, for RoboBoat 2026. After several design iterations to create a modular, inspectable, and competition–focused platform, we now aim to attempt every task at competition. While the team has prepared mechanical subsystems for object delivery and interaction, our primary emphasis this season is to develop a vehicle with reliable navigation and perception before layering on higher–risk behaviors. The design centers on two fiberglass catamaran hulls, a single structural base plate, a centralized electronics box, and a perception and autonomy stack that is simple, testable, and tailored to the RoboBoat tasks. Every major component—hulls, thrusters, electronics, and mechanisms—can be accessed and replaced quickly, enabling aggressive iteration during field testing.

1 Competition Strategy

Our main objective for RoboBoat 2026 is to field a vehicle that can *reliably* execute navigation and interaction tasks while remaining maintainable over multiple competition days. Jolorekha is designed around three priorities: (1) robust state estimation and course–level navigation, (2) clear, debuggable perception pipelines for buoys, beacons, slips, and vessels, and (3) simple but extendable mechanical mechanisms for water delivery and ball launching.

We intend to attempt all tasks, but we prioritize consistent completion of the Evacuation Route & Return, Debris Clearance, Emergency Response Sprint, and Navigate the Marina tasks. Supply Drop and high–precision object manipulation are enabled by the same water gun and ball shooter, but are treated as incremental layers on top of the core navigation stack.

1.1 Course Approach

Reliable pose estimation is the foundation of our navigation strategy. Jolorekha combines GPS data from a multi–constellation GNSS receiver with inertial measurements from an IMU, fusing them using an Extended Kalman Filter (EKF) to obtain a smooth 2D pose estimate in the map frame, following standard marine practice [1]. Each task is treated as a sequence of waypoints in a global coordinate frame, while local obstacles from onboard sensors modify the path as needed.

For obstacle representation, we maintain a local 2D occupancy grid built from LiDAR scans and camera–based detections of large objects. The grid is used by the obstacle avoidance layer and by docking behaviors; high–level path planning uses pre–defined waypoint graphs tuned to the RoboBoat field layout.

1.2 Buoy-Following Tasks

For the Evacuation Route and buoy–based segments of Debris Clearance, the ASV must detect

red and green buoys, identify gates, and localize itself relative to them.

A calibrated 1080p wide–angle RGB camera is mounted at the bow. Images are undistorted using camera intrinsics and converted to HSV color space. Color thresholds isolate red and green regions, followed by morphological closing to remove noise. Contours are extracted, and candidates are filtered by area, aspect ratio, and solidity.

When LiDAR returns are available on the same buoys, we associate vision and LiDAR detections by projecting LiDAR points into the camera frame using the known extrinsic transformation and camera intrinsics. Candidate matches are chosen by maximizing Intersection over Union (IoU) between projected LiDAR clusters and image bounding boxes. This fusion improves buoy range estimation and reduces false positives from reflected light.

Once a sequence of red and green gate buoys is localized, the ASV constructs an ordered list of gate centers. The line–of–sight (LOS) guidance algorithm described in Section 4.3 then defines intermediate waypoints between gates to generate a smooth path that respects both buoy geometry and safety clearances.

1.3 Navigate the Marina and Docking

Navigate the Marina requires Jolorekha to recognize available slips, select a target, and execute a controlled docking maneuver. Our approach combines visual slip number detection, beacon color classification, and a state machine governing approach, alignment, and final docking.

Slip numbers and dock edges are detected by a compact YOLO model trained on marina structures. Candidate slip plates are cropped and passed through an OCR pipeline to read numerical labels. Green beacons mounted near the slips are detected using the same color and intensity pipeline as task beacons. By matching slip numbers to beacon states, the autonomy layer determines the correct slip based on the chosen capability level (e.g., any free slip, green slip, or lowest–number green slip).

For motion, the docking behavior operates in one of three states: *approach*, *align*, and *final*. In the approach state, the ASV follows LOS waypoints toward a pre–docking point outside the slip. In the align state, heading is adjusted to align the boat's longitudinal axis with the slip centerline using visual feedback from dock edges. In the final state, the ASV moves forward at low speed, with a tight heading PID and proximity limits enforced by LiDAR and camera cues. A shock–absorbing bumper at the bow provides mechanical tolerance for minor contact.

1.4 Object and Water Delivery

The Supply Drop task is implemented using two mechanisms: a ball shooter and a water gun, both mounted on the central base plate. Orange vessels with triangular markers require water delivery; black vessels with plus signs require ball delivery. A vision model classifies vessel color and symbol, while coarse range is derived from bounding box size and LiDAR returns.

When a target vessel is selected, Jolorekha enters a targeting state: LOS guidance brings the ASV to a standoff distance; a servo mount orients the shooter/nozzle using pixel offsets; a short burst from the water pump or roller shooter is triggered. Because this task involves significant mechanical tuning, it is treated as lower priority relative to navigation tasks, but the mechanisms share the same mounting interfaces as the core systems.

2 Design Strategy and Mechanical Architecture

After exploring several hull and electronics layouts in early prototypes, we converged on a design focused on simplicity of assembly, accessibility for wiring and debugging, and modularity for mechanisms that may evolve between seasons. The final architecture uses two fiberglass composite hulls connected by a single structural base plate, a centralized electronics box, and four thrusters mounted directly to the plate.

2.1 Hulls

Catamarans are well–suited to RoboBoat due to their combination of high transverse stability and a wide deck area for mounting hardware. Jolorekha's hulls are symmetric for maneuverability and to simplify hydrodynamic modeling.

Each hull is built from a foam core and fiberglass composite skin: a $10\,\mathrm{mm}$ XPS foam core, two layers of 200 gsm E–glass with epoxy on the inside, and a biaxial $\pm 45^\circ$ E–glass layer on the outside for torsional stiffness. The hulls are coated with UV–resistant epoxy paint.

The hulls are attached to the base plate using aluminum brackets and stainless steel bolts. Rubber isolators between hull tops and brackets provide vibration damping and reduce stress concentrations. Mounting points are designed so that hulls can be detached without disturbing the rest of the assembly, allowing rapid transport or hull replacement.

2.2 Base Plate and Structural Layout

A single aluminum base plate spans between the hulls. It provides mounting points for thrusters, the electronics enclosure, sensor mast, bumper, ball shooter, water gun, and antenna. All external modules are bolted to the base plate with stainless hardware and can be removed independently, making the vehicle mechanically modular.

High–current wiring is routed near the center of the plate while signal lines run along the sides, reducing electromagnetic interference. Slots and holes in the plate allow water drainage and provide tie–down points for harnesses.

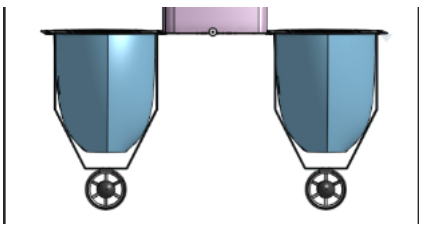

Figure 1: Side view of the hull profile and aft-mounted thrusters, illustrating draft and propulsor placement.

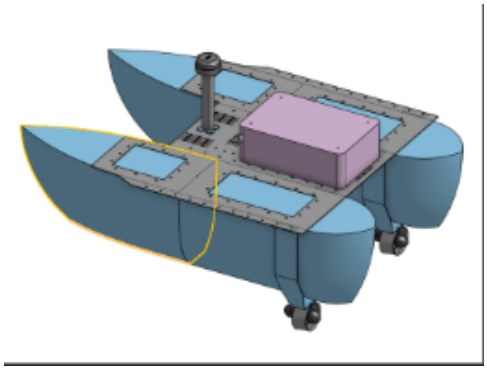

Figure 2: Isometric CAD view of Jolorekha showing the twin hulls, central base plate, electronics enclosure, and sensor mast.

2.3 Propulsion

To provide strong maneuverability while keeping control simple, Jolorekha uses four electric thrusters mounted in a rectangular configuration.

We selected T200–class brushless thrusters for their reliability and thrust margin. Thrusters are mounted in pairs near the bow and stern with thrust vectors aligned with the longitudinal axis. Adjustable brackets allow each thruster to be canted slightly outward to fine–tune turning response. The four–thruster arrangement supports differential thrust for yaw control and offers redundancy in case of partial failure.

2.4 Electronics Box and Sensor Mast

The electronics enclosure (EE box) is waterproof, compact, and easy to service. All major electronic subsystems—Jetson Nano, ESP–class microcontroller, power distribution board, and main battery—reside inside this enclosure.

We use an IP67 polymer enclosure bolted to the base plate through vibration standoffs. Removable side plates allow additional cable pass–throughs. The battery sits low, the power board below it, and the Jetson and microcontroller on side walls with heat spreaders. A panel–mount latching button on the exterior implements the emergency stop, wired to a relay that cuts ESC power.

An aluminum sensor mast mounted forward on the base plate holds the LiDAR and camera at an

elevated position to maximize field of view. The mast includes vibration–damping mounts and an attachment point for a status light beacon.

2.5 Mechanisms: Bumper, Water Gun, Ball Shooter, Antenna

A foam–rubber bumper spans the bow edge of the base plate to absorb docking impacts. The water gun consists of a 12 V diaphragm pump, short reservoir, and nozzle aligned with the camera axis. The ball shooter uses a dual–roller launcher driven by a high–RPM DC motor and a servo–actuated feed gate. A carbon–fiber mast supports the WiFi/RF antenna above the electronics to improve signal quality.

3 Electrical System

The electrical system is compact, modular, and robust against the marine environment. All high–current distribution, computing, and control electronics are centralized in the EE box; only thruster, sensor, and mechanism wiring exits through sealed cable glands.

3.1 System Overview

Fig. 3 shows a block diagram similar to the implemented architecture. A single high–capacity LiPo battery provides primary power. The Power Distribution Board (PDB) generates regulated rails for propulsion, computing, and auxiliaries, and also hosts current and voltage sensing. The Jetson Nano runs the autonomy stack under ROS 2, while an ESP–class microcontroller handles low–level tasks such as PWM generation, kill–switch monitoring, and safety interlocks.

3.2 Power Distribution and Protection

The main LiPo battery (6S, 22.2 V, 20 A h) connects to the PDB via an XT90 connector. Four fused outputs feed the ESCs. Two buck converters generate 12 V and 5 V rails. INA219 sensors

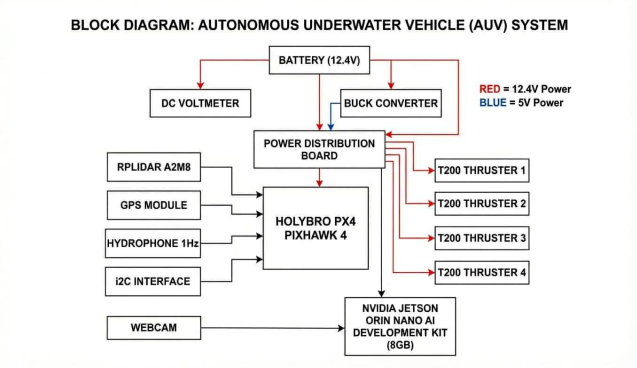

Figure 3: Electrical system block diagram for Jolorekha. A single battery feeds the PDB, which powers thrusters and electronics while interfacing with Jetson, microcontroller, and sensors.

monitor rail voltage and current for logging and protection.

The ESP microcontroller monitors pack voltage through an ADC input. When voltage drops below a configurable threshold, the autonomy stack limits its throttle and, at a lower threshold, commands a return and safe shutdown.

3.3 Emergency Stop and Interfaces

The primary E–Stop is a latching button driving a relay that interrupts power to the ESCs. In parallel, the microcontroller sets all PWM outputs to neutral when an E–Stop condition is detected. The relay is wired fail–safe: loss of power or a broken E–Stop line causes the relay to open.

Thrusters, water pump, and ball shooter are controlled by PWM and MOSFET drivers from the microcontroller. LiDAR, GPS, IMU, camera, and microphone are interfaced via UART, I^2C, SPI, CSI/USB, and analog inputs, respectively. Grounding and cable routing follow best practices to minimize EMI [6].

3.4 Power Budget and Mission Profiles

We modeled component power consumption to verify that the battery supports a full mission with margin. Fig. 4 summarizes average power per sub-

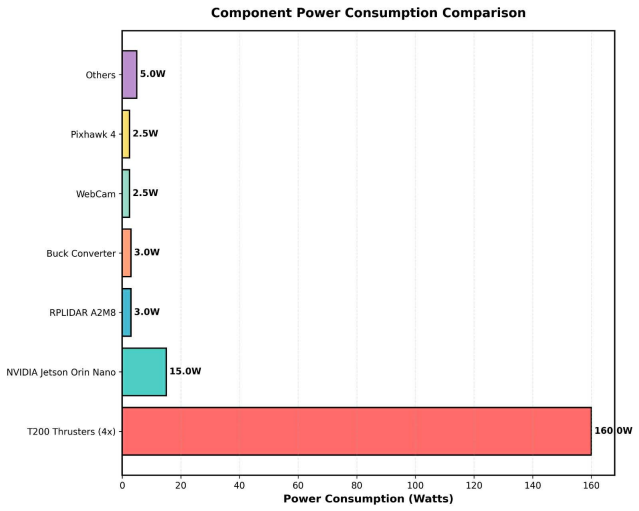

Figure 4: Component power consumption comparison. Thrusters dominate mission power draw; compute and sensors account for a small fraction.

system, illustrating that the four T200 thrusters dominate the budget.

Using these values, we simulated typical mission profiles. The stacked area plot in Fig. 5 shows thruster load distribution between forward motion, turning, and station keeping, with a highlighted E–Stop event.

Fig. 6 combines thruster and auxiliary loads into an estimated power profile over a full run, confirming that the average draw stays within the capacity of the selected battery with reserve for retries.

4 Autonomy and Algorithmic Design

Jolorekha's autonomy stack is built around reliable perception, robust state estimation, smooth guidance, and deterministic task decision–making. The stack is divided into four layers: perception (camera, LiDAR, audio), state estimation (EKF fusion), guidance and control (LOS + PID), and a task behavior layer implemented as a Behavior Tree [5].

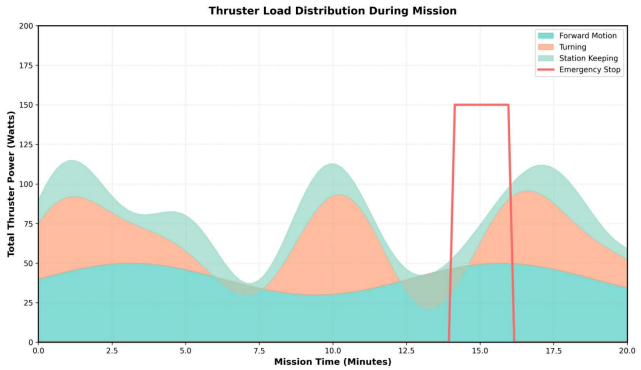

Figure 5: Thruster load distribution during a representative mission, separating forward, turning, and station–keeping contributions and showing the effect of an E–Stop.

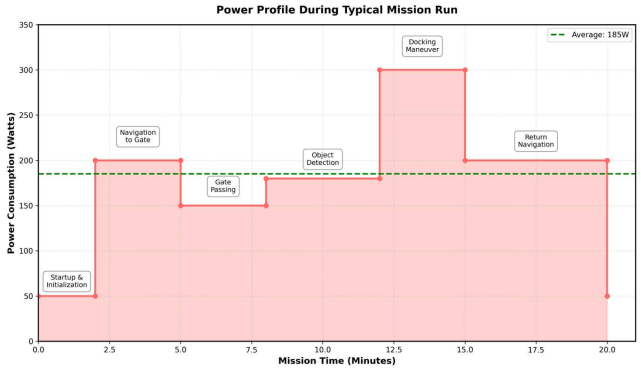

Figure 6: Estimated power profile during a typical mission run with major phases annotated.

4.1 Perception Algorithms

Perception runs at 10–15 Hz on the Jetson Nano, combining YOLOv8n detectors with classical computer vision techniques [3].

For buoy detection, the camera image is undistorted and converted to HSV. A YOLOv8n network proposes candidate bounding boxes. HSV thresholding confirms red and green color classes, and morphological closing removes noise. Contours are filtered by area and shape. LiDAR detections of buoy clusters are projected into the image frame and associated with boxes via IoU. Distances from camera geometry and LiDAR range are fused with a weighted average.

Dock slips are detected by a separate YOLO model. Candidates are cropped and passed to OCR; dock edges are extracted using Hough trans-

forms, providing slip centerlines and approach angles. Vessels for Supply Drop are classified into water–delivery or ball–delivery classes using a two–class YOLO model with range estimated from bounding box size and LiDAR.

LiDAR scans are segmented with Euclidean clustering. Small, above–water clusters populate a rolling occupancy grid used for debris clearance. For Harbor Alert, microphone audio is sampled at 8 kHz; an FFT and Hilbert envelope detect short bursts in the 200–600 Hz band. One burst maps to the Sprint zone; two bursts indicate return to the Marina.

4.2 State Estimation

An EKF fuses GPS, IMU, and magnetometer measurements using a probabilistic robotics formulation [2]. The state vector is $x = [x, y, \psi, v_x, v_y, \dot{\psi}]^T$, with prediction based on body–frame velocities and yaw rate. GPS provides absolute position at 5 Hz, while IMU data arrives at 100 Hz. Magnetometer yaw anchors heading in the absence of strong magnetic disturbances. The EKF outputs a smoothed 2D pose for guidance and mapping.

4.3 Guidance and Control

Given the current pose (x, y, ψ) and target waypoint (x_t, y_t), the LOS heading is [1]

$$\psi_d = \tan^{-1}\left(\frac{y_t - y}{x_t - x}\right).$$

Cross-track error relative to the desired path is

$$e_{ct} = (x - x_t)\sin\psi_d - (y - y_t)\cos\psi_d.$$

A corrected heading reference is

$$\psi_{ref} = \psi_d - k e_{ct}.$$

A PID controller computes yaw command

$$u_\psi = K_p e_\psi + K_d \dot{e}_\psi + K_i \int e_\psi dt,$$

where $e_\psi = \psi_{ref} - \psi$. Forward thrust command u_v is scheduled based on phase (e.g., sprint vs. docking). Differential thruster commands are $T_{left} = u_v - u_\psi, T_{right} = u_v + u_\psi$, with saturation to respect ESC limits.

4.4 Task-Specific Mission Algorithms

Each mission is a subtree in the Behavior Tree.

For the Evacuation Route, red/green buoys are detected, paired into gates, and sorted by distance. The midpoint of each gate becomes a waypoint; the boat iteratively navigates through midpoints using LOS guidance.

Debris Clearance adds LiDAR–based occupancy mapping and A* planning inside the buoy corridor, following standard grid–based planning [4]. Emergency Response Sprint detects a yellow buoy, estimates its position, generates a short circular trajectory around it, and then exits toward a finish waypoint.

Supply Drop uses vessel classification to choose water or ball delivery, moves to a standoff point, aims using pixel offsets, and fires the corresponding mechanism. Navigate the Marina uses a state machine with approach, align, and final docking stages based on slip ID, beacon color, and dock line geometry.

Harbor Alert monitoring runs in parallel with other tasks. When a valid audio pattern is detected, a high–priority selector in the Behavior Tree interrupts the current mission and transitions to the required emergency behavior.

5 Conclusion

Jolorekha combines a simple, modular mechanical platform with a focused electrical and autonomy architecture aimed at reliability first and feature growth second. The catamaran hulls and single base plate keep the structure stable and serviceable; the centralized electronics and clear power paths simplify debugging; and the autonomy stack emphasizes explainable perception and deterministic behaviors. As testing continues, we plan to refine gate following, docking robustness, and Supply Drop accuracy while maintaining the core

goal of a boat that works predictably across multiple competition days.

References

[1] T. I. Fossen, *Handbook of Marine Craft Hydrodynamics and Motion Control*. Wiley, 2011.

[2] S. Thrun, W. Burgard, and D. Fox, *Probabilistic Robotics*. MIT Press, 2005.

[3] I. Goodfellow, Y. Bengio, and A. Courville, *Deep Learning*. MIT Press, 2016.

[4] S. M. LaValle, *Planning Algorithms*. Cambridge University Press, 2006.

[5] M. Colledanchise and P. Ogren, *Behavior Trees in Robotics and AI: An Introduction*. CRC Press, 2018.

[6] H. Ott, *Electromagnetic Compatibility Engineering*. Wiley, 2009.